Materials Today Advances 6 (2020) 100050

Contents lists available at ScienceDirect

Materials Today Advances

journal homepage: www.journals.elsevier.com/materials-today-advances/

The electrifying effects of carbon-CeO_2 interfaces in (electro)catalysis

M. Melchionna [a], M. Bevilacqua [b], P. Fornasiero [a, b, *]

[a] Department of Chemical and Pharmaceutical Sciences, University of Trieste, 34127, Trieste, Italy
[b] ICCOM-CNR Trieste Associate Unit, University of Trieste, Via L. Giorgieri 1, 34127, Trieste, Italy

ARTICLE INFO

Article history:
Received 3 October 2019
Received in revised form
3 December 2019
Accepted 11 December 2019
Available online 5 February 2020

Keywords:
Carbon-ceria interfaces
Carbon-ceria-based sensors
Carbon-ceria-based electrolyzers
Carbon-ceria based fuel cells

ABSTRACT

The exceptional and unique properties of cerium dioxide have encouraged scientists to exploit this material beyond its traditional role as a promoter in automotive engines. Electrochemical processes relevant to fuel cells, electrolyzers, and sensors can be facilitated or even directly catalyzed by the CeO_2, whose redox properties are ideal for electrochemistry. However, given the insulating nature of pure ceria, the inclusion of conductive materials at the boundary with the metal oxide is necessary to boost the catalytic activity. Carbon in its various forms and morphologies is a dominant component in ceria-based electrocatalysts, significantly facilitating electron transfers and providing high surface area and improved stability. Moreover, given the improved electronic conductivity of reduced CeO_2 in the wake of the decreased grain boundary impedance, the combination with a conductive component, such as carbon, can facilitate a reduction of the ceria.

1. Introduction

1.1. Carbon-ceria interfaces. General considerations

Cerium dioxide (ceria, CeO_2) is a semi-conductive nontoxic material, well established in some catalytic applications, such as 3-way catalysts and Diesel engines, where it is used either as a promoter for the removal of polluting combustion products. In more recent years, interest in CeO_2-based material has gradually extended to other catalytic reactions, particularly related to energy applications and sustainability [1]. In this context, the preparation of ceria-based composites and hybrids at the nanoscale has propelled the use of this metal oxide in a range of new processes [2]. The primary exploitation of ceria as a component in heterogeneous catalyst packages is based on its rich redox chemistry, where the ability of the cerium to easily switch between the Ce^{3+} and Ce^{4+} oxidation states, with the concomitant tuning of the oxygen vacancies, implies a useful role as oxygen buffer [3,4]. Reducibility of metal oxides is a shared characteristic of all rare earth (RE) elements, and indeed the 3 + oxidation state is accessible to form, from nonstoichiometric reduced ceria, e.g., CeO_{2-x}, up to the corresponding sesquioxide Ce_2O_3, so that these oxides have similar reactivity fundaments and common catalytic properties, thus being used as oxygen storage materials [5]. The advantage of CeO_2 over the other RE oxides is that cerium is the most abundant of the rare earth elements [6]. Notably, the relatively nontoxic nature of CeO_2 is also a big advantage for industrial applications, also allowing it to extend its use in medicinal chemistry [7,8].

With regards to sustainability, electrochemical use of CeO_2 has had a predominant role, although typically, authors have relied on CeO_2 as support for noble metal nanoparticles that are the truly electro-active sites [9,10], and not as a direct catalyst. A serious issue with pure CeO_2 is that this metal oxide is inherently an insulator at room temperature, thus the electron transfer processes required by electrochemical set-ups could thwart its specific performance. Examples of pure CeO_2 in electrochemical applications are, therefore, still too few, while the use of a powerful strategy to circumvent this hurdle is to combine the oxide with conductive carbon phases, allowing a superior electron trafficking at the CeO_2 interface. Hence, the reducibility of ceria and access to well-defined densities of Ce^{3+} sites can potentially be tuned by employing the carbon component as an electron buffer [11,12]. Improved redox properties of the CeO_2 by contacting carbon surfaces have been already advantageously exploited in other types of catalysis, such as soot combustion [13]. The improved electronic conductivity of reduced CeO_2 in the wake of the decreased grain boundary impedance, as well as high-resolution scanning tunneling microscopy (STM) has been studied [14–16], and the combination with a conductive component, such as carbon can facilitate the reduction process of the ceria. However, although not often discussed in

* Corresponding author.
E-mail address: pfornasiero@units.it (P. Fornasiero).

https://doi.org/10.1016/j.mtadv.2019.100050

depth in most of the studies, it has become evident that such combination must be opportunely tailored so that the two phases are chemically interfaced with overlapped orbitals, such that the conductivity of the carbon is partly transferred to the oxide through diffusions of freely moving electrons.

While standard amorphous carbon can fulfill this task and is the preferred carbon phase from a cost point of view, the use of more recent carbon nanostructures, such as graphene (G), carbon nanotubes (CNTs), and carbon nanohorns (CNHs) can endow the carbon-ceria hybrids with additional functionality as also proved in several other catalytic applications [17]. It must be noted, however, that the properties of carbon-ceria nanohybrids or nanocomposites severely depend on a number of factors, and that control of the synthetic stages is of paramount importance. Electronic states and (semi)conductive behavior can vary to a large extent, and the combination of carbon and ceria phases must be tailored according to the desired purpose. Anchoring CeO_2 to (nano)carbon can proceed either by *ex-situ* or *in-situ* approaches. The former is based on a preformation of the CeO_2 nanoparticles that are subsequently attached to the prefunctionalized carbon surface [18]. In this framework, it is highly significant to control the shape and size of the CeO_2 nanoparticles (NPs), as well as the content of oxygen vacancies. For example, reduced graphene oxide (rGO) decorated with CeO_2 NPs led to the formation of nanocomposites, where the electronic transport behavior was varying between ambipolar and n-type depending on the content of oxygen vacancies in the ceria NPs (defined by the Ce^{3+}/Ce^{4+} ratio). This was attributed on the basis of current (I)-voltage (V) profiles in back-gated field-effect transistor (FET) configuration and explained in terms of a hole trapping phenomenon, where holes in RGO are electrostatically interacting (and therefore trapped) with the localized electrons of ceria (Fig. 1). Such electrons are those sitting in the *f* level of two Ce atoms where the oxygen vacancy has formed [19].

In order to fulfill their task, a critical evaluation of the functionalization step of the carbon surface is demanded. Typically, the covalent functionalization is carried out by oxidative treatment, implanting carboxylic groups that will drive the anchoring of the oxide. This step can negatively alter the electronic properties of the carbon nanostructure, while positively affecting the porosity, thus requiring a correct balance, as well as the development of alternative functionalization procedures, including noncovalent approaches [20]. As a representative example, the preparation of graphene oxide from graphene via the traditional Hummers' method [21] increases the surface area and wettability by introduction of polar carboxylated groups, but the dramatic disruption of the polyaromatic conjugation severely deteriorates the conductive properties; however, by fine-tuning the number of oxygenated groups through more sophisticated synthetic procedures, an optimum level of functionalization can be achieved for improved electrochemical behavior [22]. In the case of hybridization with the ceria phase, the functional groups on the carbon surface also aid chemical bonding for better attachment and contact between the two components [23]. Moreover, the nature of the functional groups can influence the degree of structural connection between the carbon and the ceria. This has been particularly observed in the *in-situ* synthesis of CNT-CeO_2, where the appropriate anchoring sites on CNTs, such as pyridinium hydroxide and benzoic acid, were exploited to achieve abundant adsorption of Ce species, otherwise inefficient, which were converted into CeO_2 by calcination in a second step [24,25]. Such an *in-situ* layering of the CeO_2 is a powerful strategy for optimizing the interfacing of the two phases, which is a key aspect in the electrocatalytic applications. In general, while interfaces are better achieved via *in-situ* synthesis, with resulting composites being more structurally homogenous, a major asset of the *ex-situ* path resides in the control of the crystallographic faceting of the CeO_2 nanoparticles, as well as their morphology. This is a central point in ceria-based catalytic

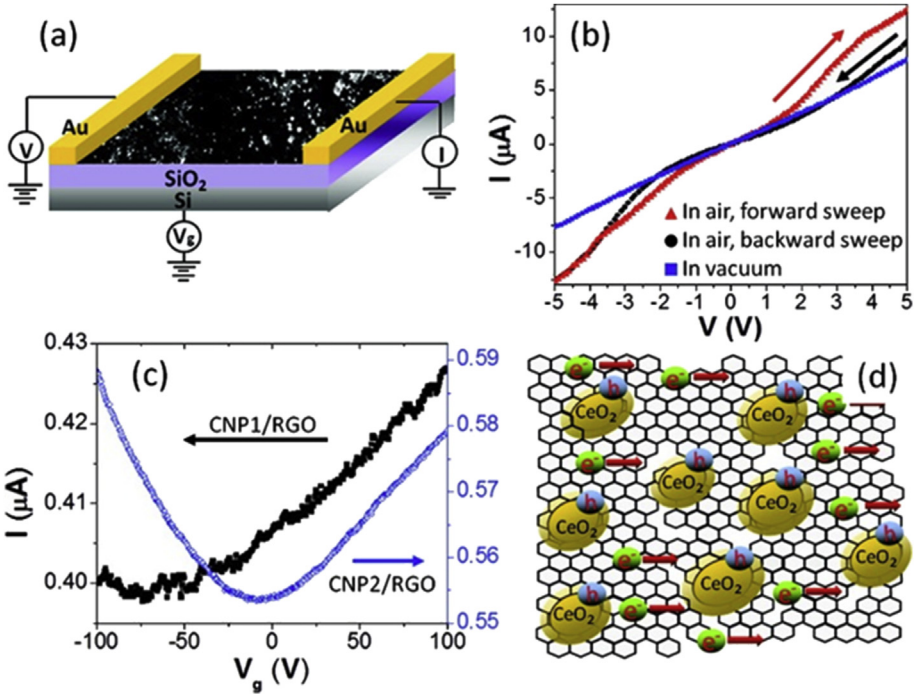

Fig. 1. (a) Schematic diagram of the rGO/CeO_2 NPs FET device structure. (b) Current (*I*)–voltage (*V*) curves of rGO/CeO_2 NPs. (c) Current (*I*) as a function of gate voltage (V_g) with $V = 1$ V. (d) Schematic illustration of the effects of oxygen vacancies created from CNP on RGO sheets. Reprinted with permission from reference 19. Copyright (2011) American Chemical Society.

applications, as the different surface energy associated with specific exposed crystallographic facet is in a tight relationship with the reactivity of the Ce ions, and in turn, the activity [26,27]. It is well known that the activity in traditional catalytic applications, such as soot combustion or CO oxidation, correlates with the exposed CeO_2 facets [28,29], and it is also to be noted that H_2O, for example, binds to CeO_2 surfaces on O vacancies and that the strength of binding depends on the specific crystal plane considered, although a clear trend is still under debate [1]. Water electrolysis can be performed by CeO_2-modified electrodes, although a high temperature is generally required, such as in solid oxide electrolysis cell (SOEC) [30,31], unless a co-catalyst is added. However, these aspects can be highly relevant in the design of ceria-based electrocatalysts for water splitting or oxygen reduction under ambient conditions, which are very popular topics in electrocatalysis, and which have already been proved with TiO_2 electrocatalysts where reducibility, defect engineering, and facet exposure is instrumental for the H_2O or O_2 binding [32–34]. With this in mind, surely the possibility to engineer the surface of nanoceria is less demanding if the nanoparticles are formed in a separate synthetic step, prior to attachment to the carbon phase. The integration of a carbon scaffold into nanoceria hybrids and composites also offers an avenue for improving the stability of the catalyst. Finally, it should be noted that many reported ceria/carbon-based electrocatalysts include additional metal components, typically transition metal nanoparticles, with a predominance of noble metals. In these cases, the resulting ternary hybrid (or composite) commonly relies on the ceria phase to function as a promoter for the catalytically active site that is the metal nanoparticle. Tailoring the structure of such ternary catalysts require a higher level of synthetic complexity, and in general, it is desirable to attain good dispersity of the transition metal species on the CeO_2, maximizing their reciprocal contact.

1.2. Electrochemical applications

1.2.1. Fuel cells

The majority of work on the exploitation of C–CeO_2 catalysts in electrochemistry has focused on anodic oxidation of alcohols, for applications in direct alcohol fuel cells (DAFCs), because of their low operative temperature. Amorphous carbon, such as carbon black (the most commonly used are Vulcan^R XC72, Ketjenblack^R EC-300, and EC-600JD, characterized by a different surface area and pore distribution) can fulfill its active support task rather well; therefore, for some time, little attention had been paid to investigate more elaborate carbon structures. Pd and Pt have been (and still are) the active metals of choice due to their high intrinsic activity and stability. In the initial reports, the role of CeO_2 in Pd- or Pt–CeO_2/C was not fully understood, although experimentally, it was recognized that the metal oxide could lead to improvement of DAFCs performance. Authors tentatively explained the improved activity to the promoted CO removal by oxidation to CO_2 catalyzed by the ceria, avoiding detrimental poisoning of the noble metal, although possible different reasons were hinted where the ceria could have a more complex function [35]. It is accepted that the electro-oxidation of an alcohol fuel, such as ethanol, by Pd catalysts is catalyzed by Pd-OH_{ads} species formed after adsorption of the hydroxide, and higher concentrations of Pd-OH_{ads} lead to faster fuel conversion [36]. The further oxidation of Pd-OH_{ads}, however, can readily proceed at anode potential >0.6 V (vs. RHE), forming inactive Pd–O species. In this frame, the advantage of including CeO_2 becomes apparent as it increases the oxidation rate of Pd to Pd-OH_{ads}, with the generation of higher concentration of active species, and therefore, improved performance in direct ethanol fuel cells (DEFCs) [37]. Pd–CeO_2/C was also recently employed with success with ethylene glycol and 1,2-propanediol as fuels [38]. Traditionally, the motivation for preferring carbon black as carbon support lies in its high surface area that facilitates dispersion of the metallic phases, although there may be issues associated with mass transport (not tuned porosity, with high microporous volumes), the stability of the carbon structure, and undesirable surface chemistry. More modern supports have been gradually become popular, such as graphene and CNTs, where the exceptional stability, chemical tunability of the surface, electron mobility, and porosity are often leading to superior performances in alcohol oxidation as compared to conventional carbon black [39,40]. Variation in the synthetic protocols was reported to address the relevant characteristics of the material, above all, interfacial contact, the active surface area of the active phase, porosity and mass transport, stability, and structural homogeneity [41–46]. Efforts have been recently devoted to devising more elaborate carbon supports, tailoring their properties on different levels: Tan et al. prepared N-doped carbon spheres with large mesoporosity via a removable SiO_2-template method and used it as a support for installing Pd NPs surrounded by CeO_2 dots. The presence of mesopores and N doping atoms acted as seeding sites for the deposition of highly dispersed Pd NPs. Moreover, mass transport phenomena benefitted from the mesoporosity of the carbon, while the known ability of N doping atoms to alter the chemical and electronic surroundings of the superficial carbon atom framework favored electrocatalytic activity in the oxidation of methanol, implying electronic participation of the carbon scaffold into the catalytic process. The authors proposed that the extensive interfacing between Pd and CeO_2 resulting from the assembly design was instrumental for the comparatively superior activity with respect to benchmark catalysts, such as PtRu/C or to CeO_2-free analogs (Fig. 2), as the ceria could decrease CO adsorption energy onto the Pd surface [47].

Despite being the very first fuel used in FC devices, hydrogen is still the most popular for a number of reasons. Indeed, while FCs based on other fuels are still mainly screened in concept studies and prototypes, Hydrogen Fuel Cells (HFC), in several variant types, are those that more frequently reach the market stage, and that already have a practical use; so CeO_2-based catalysts for Hydrogen oxidation (HOR) have been investigated by various groups. An important focus has been to replace platinum in the catalyst formulation, and palladium has been the subject of more recent research. The HOR site, in this case, was proposed to be a Pd-H_{ads} intermediate formed from chemisorption of H_2, and the role of ceria is to weaken the Pd–H bond and to aid the formation of Pd-OH_{ads} through oxygen spillover, and so improve the kinetics of H_2 oxidation [48]. Upon optimization of the interfacial contact between Pd and CeO_2, a peak power density of over 1 W cm^{-2} could recently be attained in Anion exchange membrane fuel cells (AEMFCs) under alkaline conditions, setting a new benchmark for FCs based on non-Pt catalysts [49]. The promotion effect of ceria for HOR in AEMFCs was also confirmed for M-CeO_2/C catalytic materials of other transition metals, such as Iridium, where the strong metal–support interaction (SMSI) between Ir and CeO_2 was one additional factor for the observed improved HOR, by enhancing Electrochemical Surface Area (ECSA) [50].

The oxygen reduction reaction (ORR) lies at the heart of fuel cells, being the ordinary cathodic reaction, and it is the other most investigated process for ceria-based electrocatalysts. In an attempt to mitigate the problems of long time corrosion faced by carbon black supports, Li et al. deposited CeO_2 nanoparticles on multiwalled carbon nanotubes (MWCNTs) via an *in-situ* approach based on coprecipitation of CeO_2 in the presence of oxidized MWCNTs. The composite's electrochemical stability was compared with that of Vulcan XC-72 by the accelerated aging test (AAT), confirming the significantly lower corrosion of the ceria-CNT. After the deposition of Pt NPs, the catalytic ORR was tested before and after the AAT

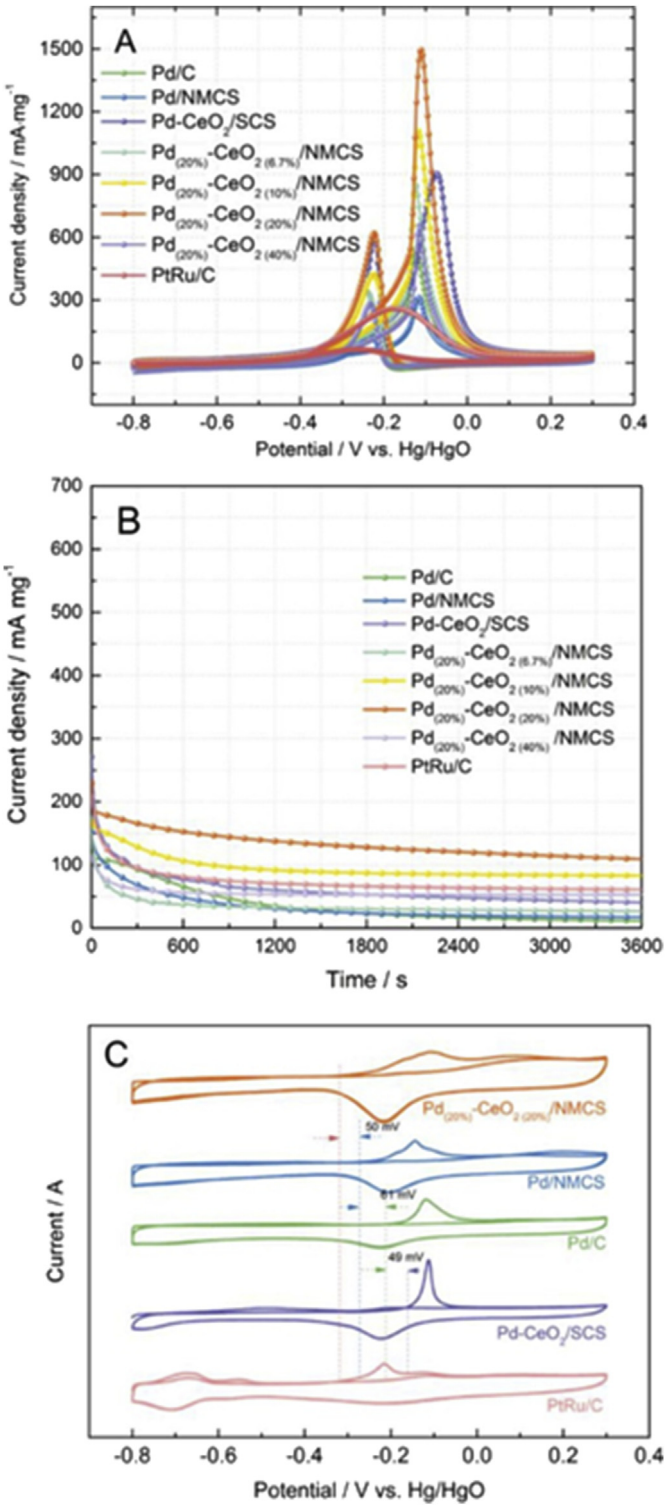

Fig. 2. Cyclic voltammetry (A) and chronoamperometry (B) curves of Pd/C, Pd/NMCS (NMCS = nitrogen-doped mesoporous carbon sphere), Pd−CeO_2/NMCS, Pd−CeO_2/SCS, and PtRu/C catalysts in N_2 saturated solution of 1.0 M KOH + 1.0 M CH_3OH. (C) CO stripping curves for different samples in N_2 saturated 1.0 M KOH solution. Reprinted with permission from reference 47. Copyright (2019) American Chemical Society.

protocol showing no decrease in activity, in contrast with the reference Pt/C catalyst. The ECSA of the two catalysts was also differently affected, with the Pt/C catalyst exhibiting decreased ECSA after 5000 cycles of AAT (Fig. 3). Such differences were explained in terms of a reduced tendency to agglomeration and to detachment when the Pt NPs were deposited on CeO_2-MWCNTs, where the Ce atoms could strongly interact with Pt due to the high content of oxygen vacancies and Ce^{3+} atoms, thus preventing aggregation. MWCNTs were instrumental in guaranteeing good conductivity, while the oxygenated functional groups could also serve as extra anchoring points for the better stabilization of the Pt NPs [51].

As noted for other electrochemical reactions, the inclusion of nitrogen atoms into the nanostructured Csp^2 pattern, even in moderate atomic percentage, alters the electronic environment of the carbon atoms adjacent to N, and this has been extensively exploited in ORR. A combination of N-doped nanocarbons with CeO_2 (and generally a transition metal) has been reported as an advanced catalyst system for ORR. The benefits of N-doping atoms was demonstrated in a few cases, for example by comparison between the doped and nondoped G in a tri-phase composite consisting of CeO_2 nanorods, Pd NPs, and three types of graphenes, where, however, the reasons for better performance with the N-doped supports were not discussed in depth [52]. Noble metal-free composites of CeO_2/N-doped reduced graphene oxide (N-rGO) were also prepared, and the synergism between the two phases emerged from the observation that the onset potential for the ORR linear sweep voltammetry (LSV), indication of the overpotential for the reduction reaction, was reduced in the nanocomposites as compared to individual N-rGO and CeO_2. In particular, the poor activity of ceria was confirmed as a result of poor conductivity, while interfacing with the graphene oxide considerably facilitated electron transfer processes to the active sites. The general ORR activity sequence observed in this particular example (CeO_2 < rGO < N-rGO < CeO_2/N-rGO) additionally underlined the importance of N-doping. The best catalyst was also superior to the benchmark Pt/C catalyst in terms of stability [53].

In the wake of the scarcity of noble metals, efforts have obviously targeted other largely available transition metal as the active center. Iron is a very appealing metal, and in a recent work by Bai et al. proper amounts of CeO_2 were used to stabilize nitrogen sources during a pyrolytic preparation of a Fe−N/C, allowing a higher density of N active sites that are decisive for ORR (Fig. 4). Moreover, the CeO_2 component could effectively reduce the H_2O_2 formed via the competitive 2-electron pathway reduction of O_2, which is detrimental for fuel cell applications [54].

The ORR catalyzed by CeO_2/C-based composites was also explored for application in other types of cells, such as Al−Air Batteries, and it was recently reported that Co_3O_4−CeO_2/C was a very active catalyst due to synergism between the two oxides [55].

1.2.2. Electrolyzers

Where the aim of a fuel cell is to power electrical energy, an electrolyzer device works in reverse, using electrical current to yield chemical products of interest. The simplest and oldest electrolyzer was applied to the splitting of H_2O_2 for the generation of H_2, a key chemical for industry, as well as a projected green energy vector that could replace current fossil fuel-based energy schemes. Hydrogen evolution reaction (HER), therefore, has a long history, and CeO_2 has found its position as a component in electrocatalyst design. As expected, noble metals play the most prominent roles as active sites, and when supported on carbon black, Pd−CeO_2 could establish a strong metal-support interaction that boosted HER with a remarkable stable current density of 15 mA cm^{-2} over 12 h of electrolysis. X-ray absorption spectroscopy (XAS) and X-ray photoelectron spectroscopy (XPS) measurements revealed the chemical nature of Pd, in contrast with Pd/C reference catalyst, where the oxidation state of Pd was 0, and the presence of ceria promotes oxidation of Pd to +2 and + 4 oxidation states. In

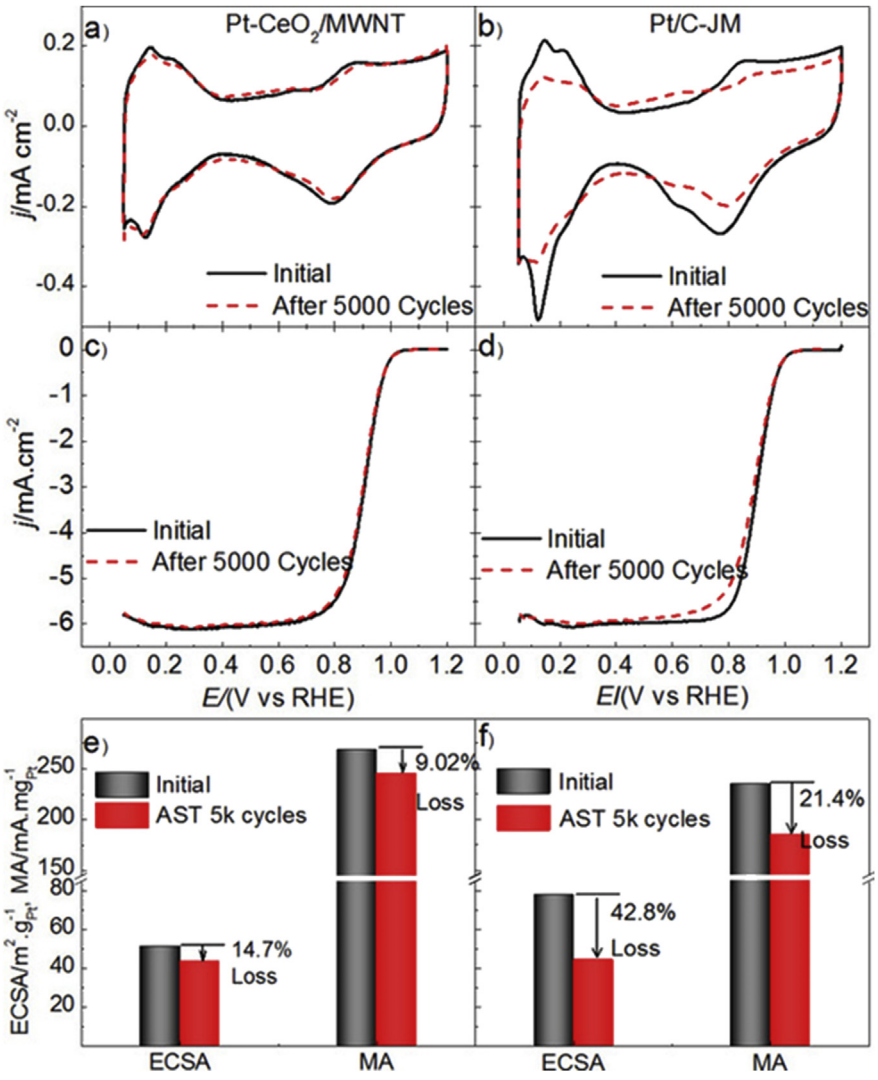

Fig. 3. Cyclic voltammograms (CVs), ORR polarization curves, and calculated electrochemical active surface areas, as well as mass-specific activity of Pt–CeO_2/MWCNT (a, c, e) and Pt/C-JM (b, d. f) before and after the accelerated aging test. Reprinted from reference 51 with permission from Elsevier.

particular, the formation of Pd–O–Ce moieties was proposed to play an important role in the HER process in alkaline media [56]. Cheaper transition metals, such as nickel, were successfully tested in combination with CeO_2. A facile chemical reduction procedure afforded the dispersion of Ni NPs on CeO_2-rGO composites that, thanks to the ceria, were grown with a smaller size distribution (~12 nm) as compared to ceria-free composite (~24 nm). Moreover, the rates of hydrogen generation were fastened by an interplay of the Ni and CeO_2 phases, where the paired 3*d* orbitals of Ni could enhance water molecule discharging and electron donating (Volmer step) and the semi-empty 5*d* orbitals of CeO_2 could facilitate the H adsorption that is important in the HER next step in alkaline media (Heyrovsky step):

$$H_2O \leftrightarrow H^+ + OH^- + e^- \rightarrow H_{ad} + OH^- \quad \textit{Volmer}$$

$$H_2O + H_{ad} + e^- \rightarrow H_2 + OH^- \quad \textit{Heyrovsky}$$

In order to maximize the synergistic effect and have an effective size control during synthesis, the CeO_2 loading must be carefully optimized. On the other hand, impedance spectroscopy demonstrated that the integration of rGO was also crucial for obtaining faster reaction rate kinetics, as a consequence of lowering of charge transfer resistance [57]. This aspect is further supported by other investigations, such as the recent work by Liu et al., who prepared CeO_2-rGO composites via the *ex-situ* approach, attaching hollow CeO_2 microspheres to GO through electrostatic interactions. A 3D network featuring porous rGO enveloping CeO_2 microspheres was finally obtained after hydrothermal treatment and compared with a more traditional CeO_2/rGO material synthesized via the *in-situ* approach in the HER catalysis (Fig. 5). It was evident how the 3D design could afford comparatively improved performance, with much lower onset potentials, indicating that structural control is of key significance [58].

An ingenious strategy for recycling a Ni/CeO_2 catalyst has been based on the reutilization of the catalyst by-product evolved from catalytic Methane Decomposition reaction (CMD). The initial catalyst Ni/CeO_2 was prepared via the sol-gel method, and after a certain operation time in CMD, the authors could retrieve poorly active Ni/CeO_2/CNT formed after accumulation at a high temperature of carbon from the methane. While inadequate for CMD, however, the material proved to be very promising for HER, where

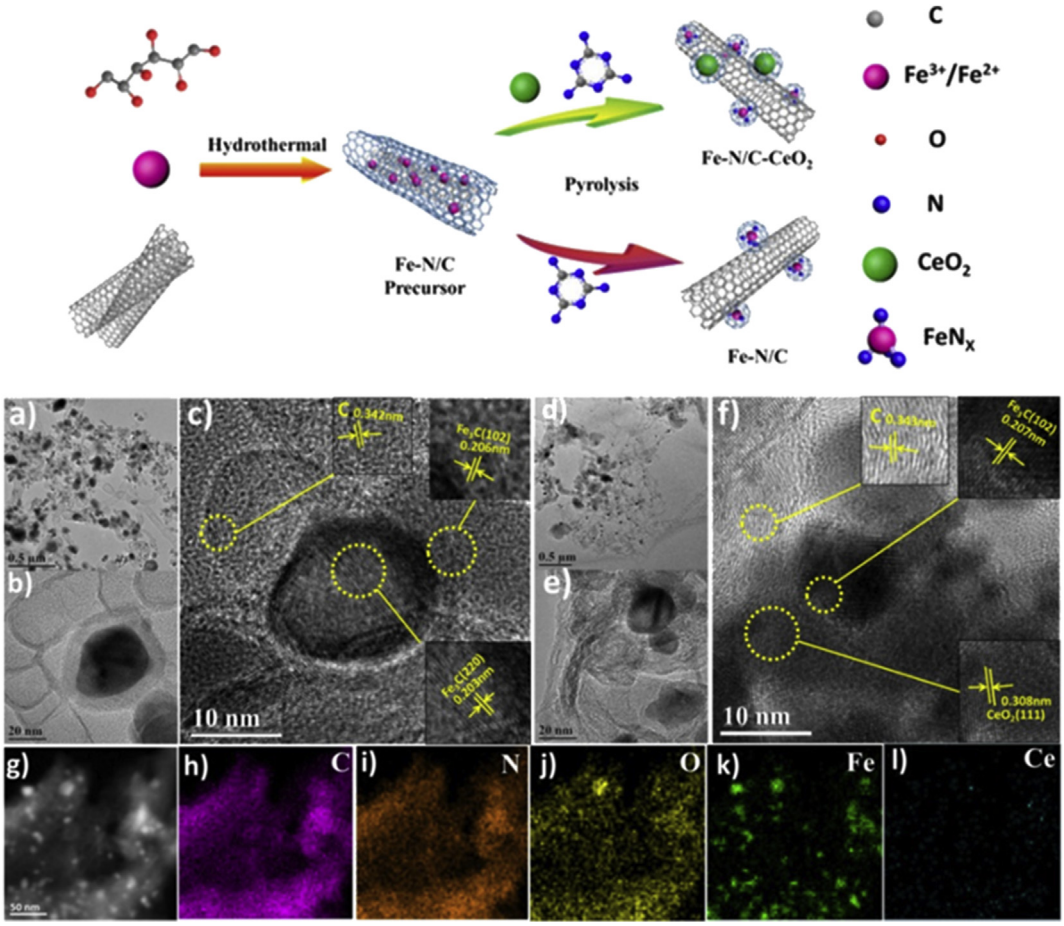

Fig. 4. Scheme of the synthesis of the final composite (top); bottom: TEM and HRTEM images of a–c) Fe–N/C and d–f) Fe–N/C–CeO_2 (1%) catalysts. g–l) The STEM and corresponding elemental mapping images of the Fe–N/C–CeO_2 (1%) catalyst. Reprinted from reference 54 with permission from Elsevier.

the CNT scaffold was crucial to increase the activity of the otherwise underperforming binary Ni/CeO_2, thus capitalizing on material sustainability [59].

Apart from H_2 production, electrolysis is a highly sustainable strategy for accessing other important chemicals. H_2O_2 is a ubiquitous molecule in an industry where it serves for multiple applications and is industrially synthesized annually in thousands of mega-tonnes via an energy-intensive process. Exploitation of ORR for the selective production of H_2O_2 is a highly appealing alternative with higher sustainability nature, and interest has rocketed over the last few years [60–63]. CeO_2 was supported on carbon black (Vulcan XC-72) for improving conductivity and surface area at reasonable cost and evaluated as an H_2O_2 electrosynthesis catalyst. It turned out that the efficiency in H_2O_2 was very high (95%), although in-depth mechanistic studies were not provided, and the reasons for such high selectivity were not clarified, calling for future additional investigations [64]. Another central industrial process is the Haber-Bosch synthesis of ammonia, which, however, is of notoriously high environmental impact from the point of view of CO_2 emission, as well as very costly. Electroreduction of N_2 is a rapidly emerging and challenging field, where the high thermodynamic stability of the N_2 is a serious hurdle that requires deep insights into catalyst design, with additional technical requirements [65]. The easily switchable redox states of Ce in CeO_2, with the formation of oxygen vacancies, have been proposed to be a promising strategy for triggering N_2 adsorption and activation, as also suggested by Density Functional Theory (DFT) calculations [66]. Integrating CeO_2 and rGO make amends for the poor conductivity of ceria, and it has been shown to be a capable catalyst for N_2 reduction to NH_3 at ambient conditions, with the encouraging ~ 17 mg h^{-1} g_{cat}^{-1} rate of NH_3 production, at a potential of −0.7 V [67].

Furthermore, CO_2 electrochemical reduction reaction (CO_2RR) is to be considered one of the most promising electrochemical processes to promote the activation of CO_2 to fuels and fine chemicals; also, in this field, CeO_2 has been successfully used as a promotor for the metal/C electrocatalysts. A representative case of study has been recently reported by Gao and coworkers [68]; in an H-type cell filled with CO_2-saturated 0.1 M $KHCO_3$ solution and operating at room temperature, the combined Au–CeO_2/C (C=Vulcan^{R}XC72) electrocatalyst showed higher activity and faradaic efficiency for CO_2RR than the separated Au/C, CeO_2/C and the reference Vulcan XC72 electrodes (Fig. 6). Experimental results supported by DFT calculations revealed the metal-oxide interface (Au–CeO_x) properties of CO_2 adsorption and activation to promote the carbon dioxide reduction process.

1.2.3. Sensors

The use of CeO_2 in (bio)sensing is well developed and applied to the detection and quantification of numerous different substrates. The biocompatibility and nontoxicity of ceria well adapt with the requirements of sensors for biological matrices, and the ceria surface is able to readily adsorb moieties of complex biomolecules, for example, by the exploitation of electrostatic interactions, and allow

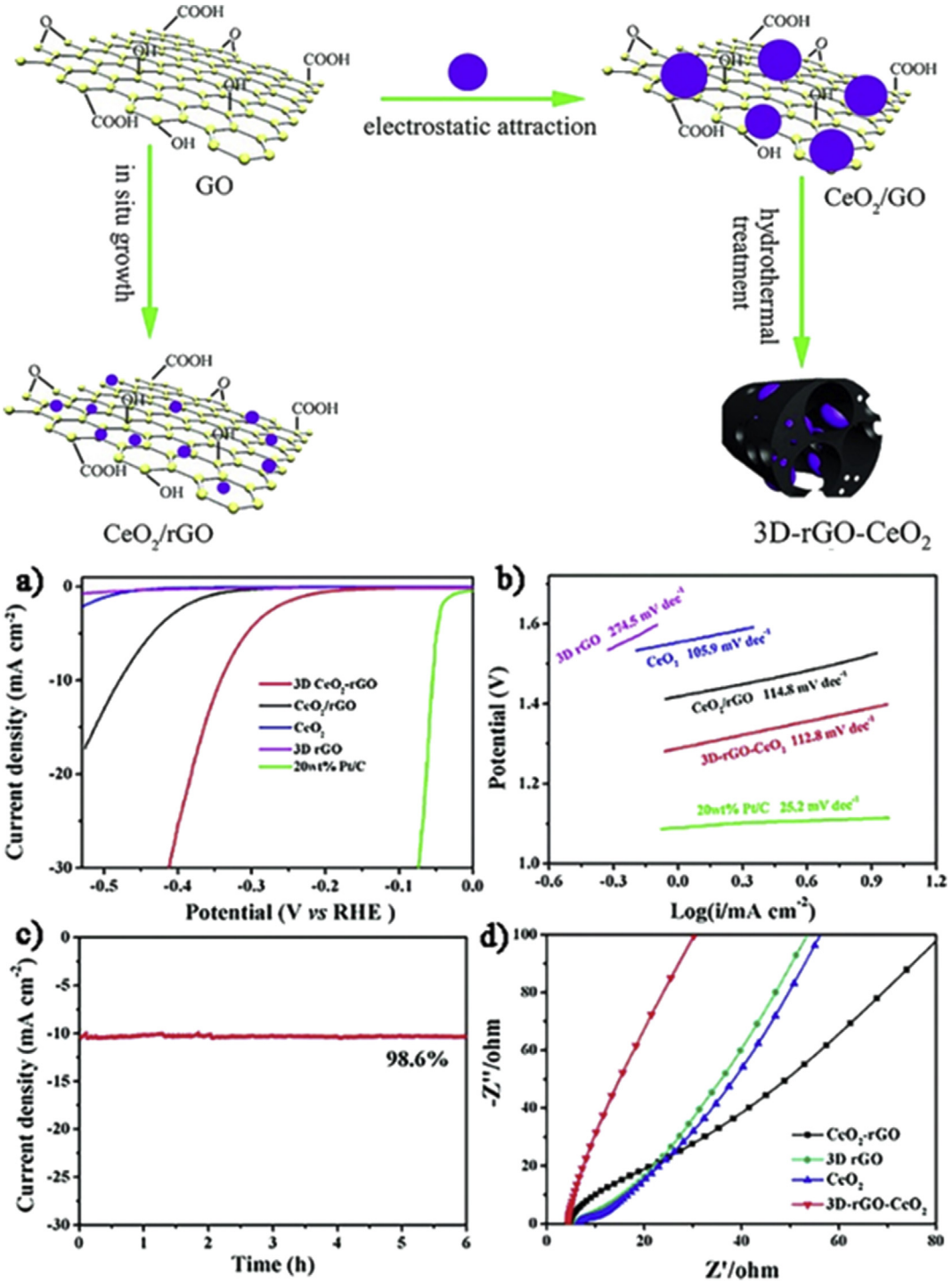

Fig. 5. Schema of the synthesis of the final composite (top); bottom: (a) Polarization curves of 3D-rGO-CeO_2, CeO_2/rGO, 3D rGO, CeO_2 hollow microspheres, and Pt/C in 1 m KOH; (b) Tafel plots of 3D-rGO-CeO_2, CeO_2/rGO, 3D rGO, CeO_2 hollow microspheres, and Pt/C; (c) Time-dependent current density curve of 3D-rGO-CeO_2 under static overpotential of 0.34 V for 6 h and (d) Electrochemical impedance spectra of CeO_2 hollow microspheres, CeO_2/rGO, 3D rGO, and 3D-rGO-CeO_2 samples. Reprinted from reference 58 with permission from Wiley and Sons.

stable immobilization and better detection. Assembly of CeO_2/single-walled carbon nanotubes/ionic liquid was, for instance, used in DNA hybridization sensing [69]. Amorphous carbon-loaded CeO_2 NPs were used together with lactate oxidase and chitosan to modify an Au electrode, and a 10-times enhancement of the current density in Cyclic voltammetry (CV) measurements in the presence of H_2O_2 10 mM was observed, remarking the higher catalytic oxidation activity of the electrode. This was relevant to the sensing of lactic acid derived from the metabolism of cancer cells, as H_2O_2 is the product of lactic acid oxidation by lactate oxidase, and therefore, an indirect measure of concentrations of this metabolite (Fig. 7). Together with sensitivity, the C/CeO_2 component afforded a lower limit of detections and linear range, respectively 300 nM and 3–300 μM [70].

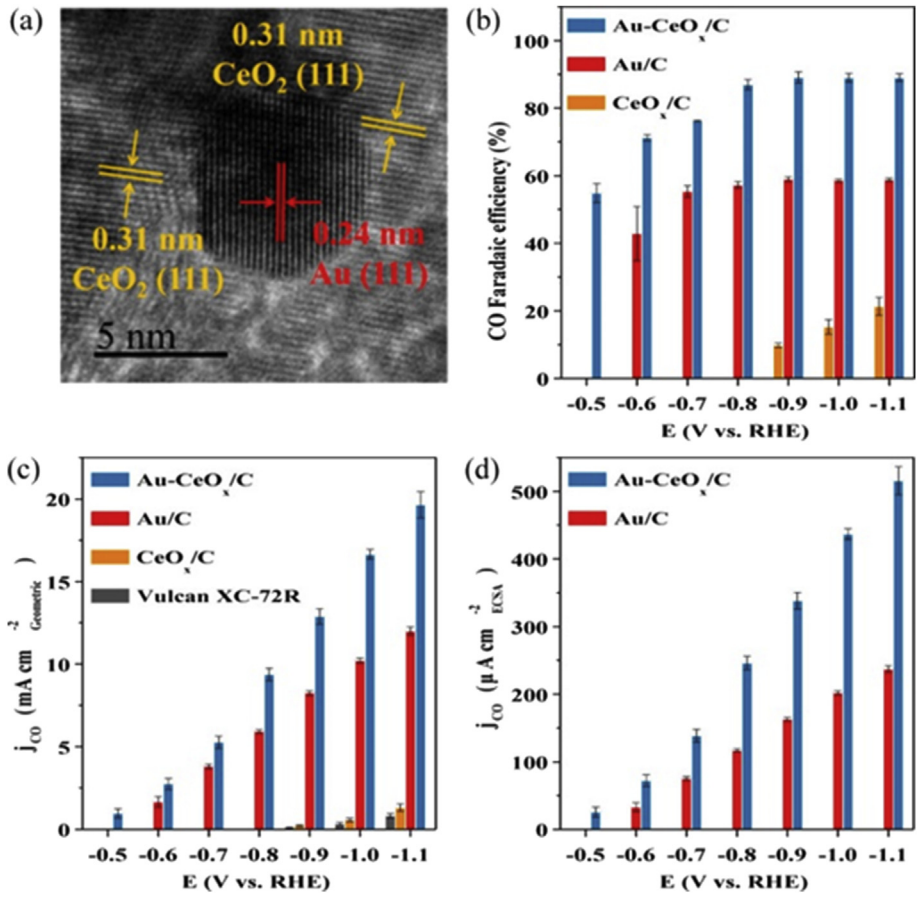

Fig. 6. (a) HRTEM image of Au−CeO_x/C catalyst. (b) Faradaic efficiency, (c) geometric partial current density, and (d) specific activity for CO production over Au/C, CeO_x/C, and Au−CeO_x/C catalysts in CO_2-saturated 0.1 M $KHCO_3$ solution and their dependence on the applied potentials. The current density for CO production over Vulcan XC-72R is also shown in (c). Reprinted with permission from reference 68. Copyright (2017) American Chemical Society.

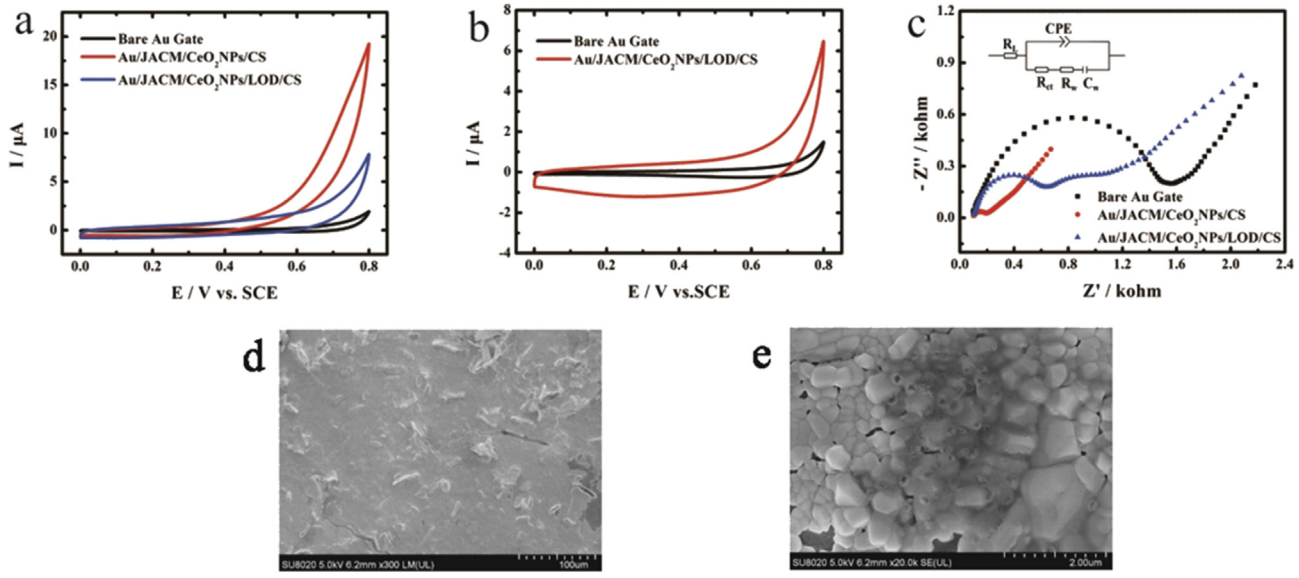

Fig. 7. a) CV of the modified electrode in 10 mM H_2O_2 in 1 × PBS (pH = 7.4). (b) CV of the modified electrode in 10 mM lactic acid in 1 × PBS (pH = 7.4). (c) Electrochemical impedance spectroscopy (EIS) of modified electrode obtained in 0.1 mM KCl solution containing 5.0 mM $[Fe(CN)_6]^{3-/4-}$ and the frequency range from 0.1 to 10^5 Hz, the DC voltage used is 0.2 V and the amplitude of 0.001 V. (d) FE-SEM image of the modified electrode surface. (e) A larger view of the figure. Reprinted from reference 70 with permission from Elsevier.

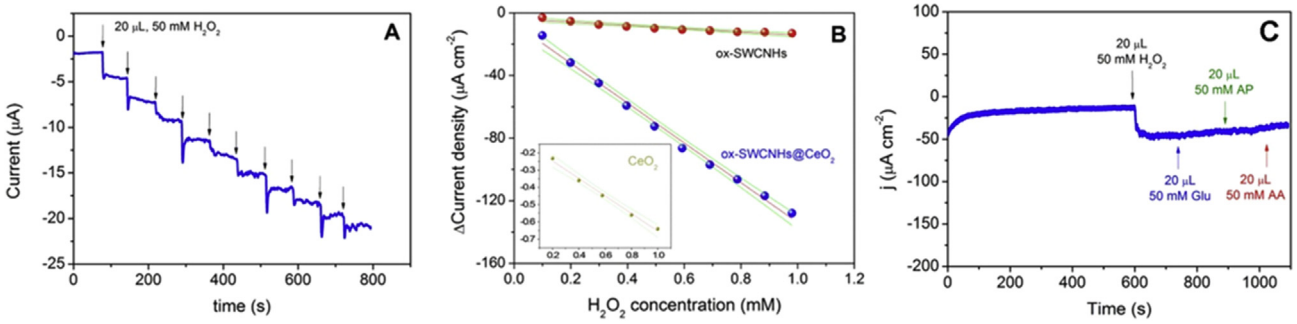

Fig. 8. (A) Amperometric plot for additions of 5.00×10^{-2} M H_2O_2 solution using ox-SWCNHs@CeO_2/GCE. Arrows indicate the addition. (B) Calibration plots obtained from the amperometric response. (C) Current-time profile for one addition of H_2O_2, followed by the same additions of ascorbic acid (AA), glucose (Glu), and acetaminophen (AP). Reprinted from reference 72 with permission from Elsevier.

On the other hand, detection and quantification of H_2O_2 is an important topic, given the ubiquity of this molecule in commercial products of daily use (cosmetics, antiseptics, hair-care, etc.), with obvious stringent regulations by governmental bodies on the permitted levels. Electrochemical sensing is simple and cheap in comparison with other more tedious or costly techniques, such as titration, fluorescence, chemiluminescence, and spectrophotometry. The affinity of CeO_2 toward H_2O_2 has motivated the employment of a ceria-modified electrode for the H_2O_2 sensing, typically exploiting catalytic oxidation reaction of H_2O_2 [71]. A nanohybrid consisting of single-walled carbon nanohorns (SWCNHs) enveloped within CeO_2 in a core-shell hierarchy proved to be an able catalyst for the electro-reduction of H_2O_2, and was successfully used as an advanced sensor, reaching a sensitivity of 160 A cm^{-2} mM^{-1} with remarkable stability. It was critical that the CeO_2 remained in its amorphous phase, as crystallization dramatically decreased the electrochemical response, likely as the result of a lower number of Ce^{3+}/Ce^{4+} ratio and OH groups. Sensing ability was also lowered by two orders of magnitude when the SWCNH was not included, pinpointing the role of the carbon phase as a conductive scaffold favoring electron transfers and kinetics. The sensor exhibited good selectivity and compatibility with complex matrices, such as milk and washing liquid (Fig. 8), an essential aspect for real device, and in addition, the cost-effectiveness is higher than typical and expensive enzyme-based H_2O_2 sensors [72].

CeO_2 was also combined with rGO through a sol-gel method the resulted in the formation of a 3D xerogel, demonstrating that even small levels of rGO into the composite composition could positively alter the sensing ability. Presumably, the large surface area of the xerogel favored mass transport that could accelerate the kinetics of the H_2O_2 reduction reaction [73]. Lead is a metal ion whose detection is crucial from a different point of view, as this metal ion is considered a notorious pollutant when found in the environment, as well as a poisoning element, when exceeding specific levels in bio-organisms. It has been shown that thrombin-binding aptamer (TBA) can perform molecular recognition and binding of Pb^{2+}. Li et al. assembled an electrochemical sensor where the TBA could be immobilized onto a glassy carbon electrode modified with a ternary composite (CeO_2—MWCNTs—$EMIMBF_4$) consisting of ceria nanoparticles, MWCNTs and ethyl-3-methylimidazolium tetrafluoroborate ($EMIMBF_4$) as an ionic liquid. The hybrid could amplify substantially the signal relative to Pb^{2+} detection [74]. The affinity of CeO_2 toward phosphate groups proved to be useful for the development of sensors for organophosphorus pesticides based on stripping voltammetric detection. The ceria nanoparticles that were proposed to enrich the concentration of the analyte at the electrode surface were combined with Au NPs as the active catalyst, while MWCNTs were integrated to enhance adsorption capacity and electrical conductivity. The synergy between these three components caused an improvement in the detection of methyl parathion (an electroactive nitroaromatic organophosphorus pesticide) affording LOD as low as 3.02×10^{-11} M [75]. Ceria/C based electrodes proved to be very versatile, and other molecules, such as hydroquinone (HQ) and catechol (CC) were recently reported to be detected and quantified with high sensitivity and selectivity thanks to the large specific area and fast electron transferring ability of the composite [76]. Very recently, ascorbic acid could be detected and quantified effectively by a CeO_2/rGO nanocomposite due to faster charge transfer allowed by the carbon phase [11].

2. Conclusions and perspectives

Cerium dioxide (ceria) has established itself as a very versatile material in many applicative fields on account of its fascinating properties. Despite the undesirable electric insulation properties, CeO_2 is a versatile material for electrochemical applications provided that opportunely modified by combination with other conductive scaffolds. In this context, the carbon in its various allotropic forms comes across as a readily available conductive partner, able to facilitate electron transfer processes and accelerate the kinetics of the particular reaction under investigation. Amorphous carbon is a safe choice, extensively employed in electrode materials for fuel cell applications due to its large abundance, low cost, and feasibility to be produced in large scales. On the other hand, carbon nanostructures (CNSs) bear the capacity to create the occurrence of new fascinating dynamics at the interface with the metal oxide phase; however, there are at least two issues that must be taken into account: (1) the synthesis of batches of CNSs with reproducible properties and structural features is still not fully harmonized among authors, particularly for large scale production (2) the CNSs must be carefully interfaced with the metal oxide with a high level of control, requiring more sophisticated synthetic efforts, and *ad hoc* prefunctionalization steps of the carbon surface. Additional emphasis should be brought on the synthetic step for the formation of the nanostructure CeO_2, which is very often neglected, but that can have strong impact on the catalytic behavior, for instance, size, shape, and morphology of the CeO_2, as well as the crystallographic faceting, play an important role in other catalytic applications, and electrocatalysis should consider this aspect more carefully. The in-depth study of the CeO_2—C interaction, with possible involvement of molecular orbitals and electron injections, is worth being investigated in future work. Finally, given the narrow bandgap of CeO_2, which is able to absorb visible light, and the crystal planes engineering, CeO_2 is a valuable material for

photocatalytic applications [77]. As an important development, a number of CeO_2-carbon-based materials, such as CeO_2-graphene and CeO_2-graphitic carbon nitride (g-C_3N_4), have been explored for their applications in photocatalytic water splitting and CO_2 reduction. CeO_2/g-C_3N_4 material had attracted much attention and a lot of characterizations, including photoelectrochemical measurements, were performed to show that the interfacial interactions were of great significance in separation and transfer of photoexcited charge carriers of CeO_2/g-C_3N_4 catalyst [78]. On the basis of the above concepts, the extension of CeO_2–C composites to photoelectrochemical applications are expected to become more and more relevant.

Declaration of competing interest

The authors declare that they have no known competing financial interests or personal relationships that could have appeared to influence the work reported in this paper.

Acknowledgements

MM kindly acknowledges the “Microgrants” project funded by the University of Trieste.

References

[1] T. Montini, M. Melchionna, M. Monai, P. Fornasiero, Fundamentals and catalytic applications of CeO_2-based materials, Chem. Rev. 116 (2016) 5987–6041.
[2] M. Melchionna, P. Fornasiero, The role of ceria-based nanostructured materials in energy applications, Mater, Today 17 (2014) 349–357.
[3] S.Y. Christou, C.N. Costa, A.M. Efstathiou, A two-step reaction mechanism of oxygen release from Pd/CeO_2: mathematical modelling based on step gas concentration experiments, Top. Catal. 30 (2004) 325–331.
[4] C. Sun, H. Li, L. Chen, Nanostructured ceria-based materials: synthesis, properties, and applications, Energy Environ. Sci. 5 (2012) 8475–8505.
[5] S. Bernal, G. Blanco, J.J. Calvino, J.A.P. Omil, J.M. Pintado, Some major aspects of the chemical behavior of rare earth oxides: an overview, J. Alloy. Comp. 408–412 (2006) 496–502.
[6] N. Haque, A. Hughes, S. Lim, C. Vernon, Rare earth elements: overview of mining, mineralogy, uses, sustainability and environmental impact, Resources 3 (2014) 614–635.
[7] J. Chen, S. Patil, S. Seal, J.F. McGinnis, Nat. Nanotechnol. 1 (2006) 142.
[8] D. Oró, T. Yudina, G. Fernández-Varo, E. Casals, V. Reichenbach, G. Casals, B. González de la Presa, S. Sandalinas, S. Carvajal, V. Puntes, W. Jiménez, Cerium oxide nanoparticles reduce steatosis, portal hypertension and display anti-inflammatory properties in rats with liver fibrosis, J. Hepatol. 64 (2016) 691–698.
[9] Y. Wang, Z. Chen, P. Han, Y. Du, Z. Gu, X. Xu, G. Zheng, Single-atomic Cu with multiple oxygen vacancies on ceria for electrocatalytic CO_2 reduction to CH_4, ACS Catal. 8 (2018) 7113–7119.
[10] V. Papaefthimiou, M. Shishkin, D.K. Niakolas, M. Athanasiou, Y.T. Law, R. Arrigo, D. Teschner, M. Hävecker, A. Knop-Gericke, R. Schlögl, T. Ziegler, S.G. Neophytides, S. Zafeiratos, On the active surface state of nickel-ceria solid oxide fuel cell anodes during Methane electrooxidation, Adv. Energy Mater. 3 (2013) 762–769.
[11] A. Murali, Y.P. Lan, P.K. Sarswat, M.L. Free, Synthesis of CeO_2/reduced graphene oxide nanocomposite for electrochemical determination of ascorbic acid and dopamine and for photocatalytic applications, Mater, Today Chem 12 (2019) 222–232.
[12] C. Fang, D. Zhang, L. Shi, R. Gao, H. Li, L. Ye, J. Zhang, Highly dispersed CeO_2 on carbon nanotubes for selective catalytic reduction of NO with NH_3, Catal Sci Technol 3 (2013) 803–811.
[13] E. Aneggi, V. Rico-Perez, C. de Leitenburg, S. Maschio, L. Soler, J. Llorca, A. Trovarelli, Ceria–Zirconia particles wrapped in a 2D carbon envelope: improved low-temperature oxygen transfer and oxidation activity, Angew. Chem. Int. Ed. 54 (2015) 14040–14043.
[14] E.B. Lavik, I. Kosacki, H.L. Tuller, Y.M. Chiang, J.Y. Ying, Nonstoichiometry and electrical conductivity of nanocrystalline CeO_{2-x}, J. Electroceram. 1 (1997) 7–14.
[15] A. Tschöpe, Interface defect chemistry and effective conductivity in polycrystalline cerium oxide, J. Electroceram. 14 (2005) 5–23.
[16] F. Esch, S. Fabris, L. Zhou, T. Montini, C. Africh, P. Fornasiero, G. Comelli, R. Rosei, Electron localization determines defect formation on ceria substrates, Science 309 (2005) 752–755.
[17] A.B. Dongil, L. Pastor-Pérez, N. Escalona, A. Sepúlveda-Escribano, Carbon nanotube-supported Ni–CeO_2 catalysts. Effect of the support on the catalytic performance in the low-temperature WGS reaction, Carbon 101 (2016) 296–304.
[18] D. Eder, Carbon Nanotube–Inorganic hybrids, Chem. Rev. 110 (2010) 1348–1385.
[19] D. Joung, V. Singh, S. Park, A. Schulte, S. Seal, S.I. Khondaker, Anchoring ceria nanoparticles on reduced graphene oxide and their electronic transport properties, J. Phys. Chem. C 115 (2011) 24494–24500.
[20] M. Melchionna, M. Prato, Functionalizing carbon nanotubes: an indispensable step towards applications, ECS J. Solid State Sci. Technol. 2 (2013) M3040–M3045.
[21] W.S. Hummers, R.E. Offeman, Preparation of graphitic oxide, J. Am. Chem. Soc. 80 (1958), 1339-1339.
[22] A. Lenarda, A. Bakandritsos, M. Bevilacqua, C. Tavagnacco, M. Melchionna, A. Naldoni, T. Steklý, M. Otyepka, R. Zbořil, P. Fornasiero, Selective functionalization blended with scaffold conductivity in graphene acid promotes H_2O_2 electrochemical sensing, ACS Omega 4 (2019) 19944–19952.
[23] A. Beltram, M. Melchionna, T. Montini, L. Nasi, R.J. Gorte, M. Prato, P. Fornasiero, Improved activity and stability of Pd@CeO_2 core-shell catalysts hybridized with multi-walled carbon nanotubes in the water gas shift reaction, Catal. Today 253 (2015) 142–148.
[24] D. Zhang, C. Pan, L. Shi, L. Huang, J. Fang, H. Fu, A highly reactive catalyst for CO oxidation: CeO_2 nanotubes synthesized using carbon nanotubes as removable templates, Microporous Mesoporous Mater. 117 (2009) 193–200.
[25] M. Melchionna, A. Beltram, A. Stopin, T. Montini, R.W. Lodge, A.N. Khlobystov, D. Bonifazi, M. Prato, P. Fornasiero, Magnetic shepherding of nanocatalysts through hierarchically-assembled Fe-filled CNTs hybrids, Appl. Catal. B Environ. 227 (2018) 356–365.
[26] A. Trovarelli, J. Llorca, Ceria catalysts at nanoscale: how do crystal shapes shape catalysis? ACS Catal. 7 (2017) 4716–4735.
[27] Y. Ma, W. Gao, Z. Zhang, S. Zhang, Z. Tian, Y. Liu, J.C. Ho, Y. Qu, Regulating the surface of nanoceria and its applications in heterogeneous catalysis, Surf. Sci. Rep. 73 (2018) 1–36.
[28] K. Zhou, X. Wang, X. Sun, Q. Peng, Y. Li, Enhanced catalytic activity of ceria nanorods from well-defined reactive crystal planes, J. Catal. 229 (2005) 206–212.
[29] E. Aneggi, C. de Leitenburg, J. Llorca, A. Trovarelli, Higher activity of Diesel soot oxidation over polycrystalline ceria and ceria–zirconia solid solutions from more reactive surface planes, Catal. Today 197 (2012) 119–126.
[30] C. Zhang, Y. Yu, M.E. Grass, C. Dejoie, W. Ding, K. Gaskell, N. Jabeen, Y.P. Hong, A. Shavorskiy, H. Bluhm, W.-X. Li, G.S. Jackson, Z. Hussain, Z. Liu, B.W. Eichhorn, Mechanistic studies of water electrolysis and hydrogen electro-oxidation on high temperature ceria-based solid oxide electrochemical cells, J. Am. Chem. Soc. 135 (2013) 11572–11579.
[31] H.P. Dasari, K. Ahn, S.-Y. Park, H.-I. Ji, K.J. Yoon, B.-K. Kim, H.-J. Je, H.-W. Lee, J.-H. Lee, Hydrogen production from water-splitting reaction based on RE-doped ceria–zirconia solid-solutions, Int. J. Hydrogen Energy 38 (2013) 6097–6103.
[32] J. Swaminathan, R. Subbiah, V. Singaram, Defect-rich metallic titania ($TiO_{1.23}$)—an efficient hydrogen evolution catalyst for electrochemical water splitting, ACS Catal. 6 (2016) 2222–2229.
[33] G. Valenti, A. Boni, M. Melchionna, M. Cargnello, L. Nasi, G. Bertoni, R.J. Gorte, M. Marcaccio, S. Rapino, M. Bonchio, P. Fornasiero, M. Prato, F. Paolucci, Co-axial heterostructures integrating palladium/titanium dioxide with carbon nanotubes for efficient electrocatalytic hydrogen evolution, Nat. Commun. 7 (2016) 13549.
[34] D.-N. Pei, L. Gong, A.-Y. Zhang, X. Zhang, J.-J. Chen, Y. Mu, H.-Q. Yu, Defective titanium dioxide single crystals exposed by high-energy {001} facets for efficient oxygen reduction, Nat. Commun. 6 (2015) 8696.
[35] M.A. Scibioh, S.-K. Kim, E.A. Cho, T.-H. Lim, S.-A. Hong, H.Y. Ha, Pt-CeO_2/C anode catalyst for direct methanol fuel cells, Appl. Catal. B Environ. 84 (2008) 773–782.
[36] Z.X. Liang, T.S. Zhao, J.B. Xu, L.D. Zhu, Mechanism study of the ethanol oxidation reaction on palladium in alkaline media, Electrochim. Acta 54 (2009) 2203–2208.
[37] V. Bambagioni, C. Bianchini, Y. Chen, J. Filippi, P. Fornasiero, M. Innocenti, A. Lavacchi, A. Marchionni, W. Oberhauser, F. Vizza, Energy efficiency enhancement of ethanol electrooxidation on Pd–CeO_2/C in passive and active polymer electrolyte-membrane fuel cells, ChemSusChem 5 (2012) 1266–1273.
[38] A. Lenarda, M. Bellini, A. Marchionni, H.A. Miller, T. Montini, M. Melchionna, F. Vizza, M. Prato, P. Fornasiero, Nanostructured carbon supported Pd-ceria as anode catalysts for anion exchange membrane fuel cells fed with polyalcohols, Inorg. Chim. Acta 470 (2018) 213–220.
[39] S. Liao, K.-A. Holmes, H. Tsaprailis, V.I. Birss, High performance PtRuIr catalysts supported on carbon nanotubes for the anodic oxidation of methanol, J. Am. Chem. Soc. 128 (2006) 3504–3505.
[40] Y.L. Hsin, K.C. Hwang, C.-T. Yeh, Poly(vinylpyrrolidone)-Modified graphite carbon nanofibers as promising supports for PtRu catalysts in direct methanol fuel cells, J. Am. Chem. Soc. 129 (2007) 9999–10010.
[41] Z. Sun, X. Wang, Z. Liu, H. Zhang, P. Yu, L. Mao, Pt–Ru/CeO_2/Carbon nanotube nanocomposites: an efficient electrocatalyst for direct methanol fuel cells, Langmuir 26 (2010) 12383–12389.
[42] D.-J. Guo, Z.-H. Jing, A novel co-precipitation method for preparation of Pt-CeO_2 composites on multi-walled carbon nanotubes for direct methanol fuel cells, J. Power Sources 195 (2010) 3802–3805.

[43] X. Lou, J. Chen, M. Wang, J. Gu, P. Wu, D. Sun, Y. Tang, Carbon nanotubes supported cerium dioxide and platinum nanohybrids: layer-by-layer synthesis and enhanced electrocatalytic activity for methanol oxidation, J. Power Sources 287 (2015) 203–210.
[44] S. Yu, Q. Liu, W. Yang, K. Han, Z. Wang, H. Zhu, Graphene–CeO_2 hybrid support for Pt nanoparticles as potential electrocatalyst for direct methanol fuel cells, Electrochim, Acta 94 (2013) 245–251.
[45] W. Yuan, J. Zhang, P.K. Shen, C.M. Li, S.P. Jiang, Self-assembled CeO_2 on carbon nanotubes supported Au nanoclusters as superior electrocatalysts for glycerol oxidation reaction of fuel cells, Electrochim. Acta 190 (2016) 817–828.
[46] L. Zhang, Y. Shen, One-pot synthesis of platinum–ceria/graphene nanosheet as advanced electrocatalysts for alcohol oxidation, ChemElectroChem 2 (2015) 887–895.
[47] Q. Tan, C. Shu, J. Abbott, Q. Zhao, L. Liu, T. Qu, Y. Chen, H. Zhu, Y. Liu, G. Wu, Highly dispersed Pd-CeO_2 nanoparticles supported on N-doped core–shell structured mesoporous carbon for methanol oxidation in alkaline media, ACS Catal. 9 (2019) 6362–6371.
[48] H.A. Miller, A. Lavacchi, F. Vizza, M. Marelli, F. Di Benedetto, F. D'Acapito, Y. Paska, M. Page, D.R. Dekel, A Pd/C-CeO_2 anode catalyst for high-performance platinum-free anion exchange membrane fuel cells, Angew. Chem. Int. Ed. 55 (2016) 6004–6007.
[49] M. Bellini, M.V. Pagliaro, A. Lenarda, P. Fornasiero, M. Marelli, C. Evangelisti, M. Innocenti, Q. Jia, S. Mukerjee, J. Jankovic, L. Wang, J.R. Varcoe, C.B. Krishnamurthy, I. Grinberg, E. Davydova, D.R. Dekel, H.A. Miller, F. Vizza, Palladium–ceria catalysts with enhanced alkaline hydrogen oxidation activity for anion exchange membrane fuel cells, ACS Appl. Energy Mater. 2 (2019) 4999–5008.
[50] B. Qin, H. Yu, J. Chi, J. Jia, X. Gao, D. Yao, B. Yi, Z. Shao, A novel Ir/CeO_2–C nanoparticle electrocatalyst for the hydrogen oxidation reaction of alkaline anion exchange membrane fuel cells, RSC Adv. 7 (2017) 31574–31581.
[51] Y. Li, X. Zhang, S. Wang, G. Sun, Durable platinum-based electrocatalyst supported by multiwall carbon nanotubes modified with CeO_2, ChemElectroChem 5 (2018) 2442–2448.
[52] J.C. Carrillo-Rodríguez, S. García-Mayagoitia, R. Pérez-Hernández, M.T. Ochoa-Lara, F. Espinosa-Magaña, F. Fernández-Luqueño, P. Bartolo-Pérez, I.L. Alonso-Lemus, F.J. Rodríguez-Varela, Evaluation of the novel PdCeO_2-NR electrocatalyst supported on N-doped graphene for the oxygen reduction reaction and its use in a microbial fuel cell, J. Power Sources 414 (2019) 103–114.
[53] S. Soren, B.D. Mohaptra, S. Mishra, A.K. Debnath, D.K. Aswal, K.S.K. Varadwaj, P. Parhi, Nano ceria supported nitrogen doped graphene as a highly stable and methanol tolerant electrocatalyst for oxygen reduction, RSC Adv. 6 (2016) 77100–77104.
[54] S. Bai, X. Zhang, Y. Yu, J. Li, Y. Yang, H. Wei, H. Chu, Fabricating nitrogen-rich Fe–N/C electrocatalysts through CeO_2-assisted pyrolysis for enhanced oxygen reduction reaction, ChemElectroChem 6 (2019) 4040–4048.
[55] K. Liu, X. Huang, H. Wang, F. Li, Y. Tang, J. Li, M. Shao, Co_3O_4–CeO_2/C as a highly active electrocatalyst for oxygen reduction reaction in Al–air Batteries, ACS Appl. Mater. Interfaces 8 (2016) 34422–34430.
[56] T. Gao, J. Yang, M. Nishijima, H.A. Miller, F. Vizza, H. Gu, H. Chen, Y. Hu, Z. Jiang, L. Wang, L. Shuai, M. Qiu, C. Lei, A. Zhang, Y. Hou, Q. He, Evidence of the strong metal support interaction in a palladium-ceria hybrid electrocatalyst for enhancement of the hydrogen evolution reaction, J. Eletrochem. Soc. 165 (2018) F1147–F1153.
[57] M. Zhiani, S. Kamali, Synergistic effect of ceria on the structure and hydrogen evolution activity of nickel nanoparticles grown on reduced graphene oxide, J. Mater. Chem. 5 (2017) 8108–8116.
[58] M. Liu, Z. Ji, X. Shen, H. Zhou, J. Zhu, X. Xie, C. Song, X. Miao, L. Kong, G. Zhu, An electrocatalyst for a hydrogen evolution reaction in an alkaline medium: three-dimensional graphene supported CeO_2 hollow microspheres, Eur. J. Inorg. Chem. 2018 (2018) 3952–3959.
[59] C. Zhang, W. Zhang, N.E. Drewett, X. Wang, S.J. Yoo, H. Wang, T. Deng, J.-G. Kim, H. Chen, K. Huang, S. Feng, W. Zheng, Integrating catalysis of Methane decomposition and electrocatalytic hydrogen evolution with Ni/CeO_2 for improved hydrogen production efficiency, ChemSusChem 12 (2019) 1000–1010.
[60] D. Iglesias, A. Giuliani, M. Melchionna, S. Marchesan, A. Criado, L. Nasi, M. Bevilacqua, C. Tavagnacco, F. Vizza, M. Prato, P. Fornasiero, N-doped graphitized carbon nanohorns as a forefront electrocatalyst in highly selective O_2 reduction to H_2O_2, Chem 4 (2018) 106–123.
[61] M. Melchionna, P. Fornasiero, M. Prato, The rise of hydrogen peroxide as the main product by metal-free catalysis in oxygen reductions, Adv. Mater. 31 (2019), 1802920.
[62] S. Siahrostami, A. Verdaguer-Casadevall, M. Karamad, D. Deiana, P. Malacrida, B. Wickman, M. Escudero-Escribano, E.A. Paoli, R. Frydendal, T.W. Hansen, I. Chorkendorff, I.E.L. Stephens, J. Rossmeisl, Enabling direct H_2O_2 production through rational electrocatalyst design, Nat. Mater. 12 (2013) 1137.
[63] R. Shen, W. Chen, Q. Peng, S. Lu, L. Zheng, X. Cao, Y. Wang, W. Zhu, J. Zhang, Z. Zhuang, C. Chen, D. Wang, Y. Li, High-concentration single atomic Pt sites on hollow CuS_x for selective O_2 reduction to H_2O_2 in acid solution, Chem 5 (2019) 2099–2110.
[64] V.S. Pinheiro, E.C. Paz, L.R. Aveiro, L.S. Parreira, F.M. Souza, P.H.C. Camargo, M.C. Santos, Ceria high aspect ratio nanostructures supported on carbon for hydrogen peroxide electrogeneration, Electrochim. Acta 259 (2018) 865–872.
[65] A.R. Singh, B.A. Rohr, M.J. Statt, J.A. Schwalbe, M. Cargnello, J.K. Nørskov, Strategies toward selective electrochemical ammonia synthesis, ACS Catal. 9 (2019) 8316–8324.
[66] H. Xie, H. Wang, Q. Geng, Z. Xing, W. Wang, J. Chen, L. Ji, L. Chang, Z. Wang, J. Mao, Oxygen vacancies of Cr-doped CeO_2 nanorods that efficiently enhance the performance of electrocatalytic N2 fixation to NH3 under ambient conditions, Inorg. Chem. 58 (2019) 5423–5427.
[67] H. Xie, Q. Geng, X. Li, T. Wang, Y. Luo, A.A. Alshehri, K.A. Alzahrani, B. Li, Z. Wang, J. Mao, Ceria-reduced graphene oxide nanocomposite as an efficient electrocatalyst towards artificial N_2 conversion to NH_3 under ambient conditions, Chem. Commun. 55 (2019) 10717–10720.
[68] D. Gao, Y. Zhang, Z. Zhou, F. Cai, X. Zhao, W. Huang, Y. Li, J. Zhu, P. Liu, F. Yang, G. Wang, X. Bao, Enhancing CO_2 electroreduction with the metal–oxide interface, J. Am. Chem. Soc. 139 (2017) 5652–5655.
[69] W. Zhang, T. Yang, X. Zhuang, Z. Guo, K. Jiao, An ionic liquid supported CeO_2 nanoshuttles–carbon nanotubes composite as a platform for impedance DNA hybridization sensing, Biosens. Bioelectron. 24 (2009) 2417–2422.
[70] Y. Bi, L. Ye, Y. Mao, L. Wang, H. Qu, J. Liu, L. Zheng, Porous carbon supported nanoceria derived from one step in situ pyrolysis of Jerusalem artichoke stalk for functionalization of solution-gated graphene transistors for real-time detection of lactic acid from cancer cell metabolism, Biosens. Bioelectron. 140 (2019) 111271.
[71] S.K. Ujjain, A. Das, G. Srivastava, P. Ahuja, M. Roy, A. Arya, K. Bhargava, N. Sethy, S.K. Singh, R.K. Sharma, M. Das, Nanoceria based electrochemical sensor for hydrogen peroxide detection, Biointerphases 9 (2014), 031011.
[72] M.V. Bracamonte, M. Melchionna, A. Giuliani, L. Nasi, C. Tavagnacco, M. Prato, P. Fornasiero, H_2O_2 sensing enhancement by mutual integration of single walled carbon nanohorns with metal oxide catalysts: the CeO_2 case, Sens. Actuators B Chem. 239 (2017) 923–932.
[73] S.K. Jha, C.N. Kumar, R.P. Raj, N.S. Jha, S. Mohan, Synthesis of 3D porous CeO_2/reduced graphene oxide xerogel composite and low level detection of H_2O_2, Electrochim. Acta 120 (2014) 308–313.
[74] Y. Li, X.-R. Liu, X.-H. Ning, C.-C. Huang, J.-B. Zheng, J.-C. Zhang, An ionic liquid supported CeO_2 nanoparticles–carbon nanotubes composite-enhanced electrochemical DNA-based sensor for the detection of Pb^{2+}, J. Pharm. Anal. 1 (2011) 258–263.
[75] J. Dong, X. Wang, F. Qiao, P. Liu, S. Ai, Highly sensitive electrochemical stripping analysis of methyl parathion at MWCNTs–CeO_2–Au nanocomposite modified electrode, Sens. Actuators B Chem. 186 (2013) 774–780.
[76] D. Liu, F. Li, D. Yu, J. Yu, Y. Ding, Mesoporous carbon and ceria nanoparticles composite modified electrode for the simultaneous determination of hydroquinone and catechol, Nanomaterials 9 (2019) 54.
[77] P. Li, Y. Zhou, Z. Zhao, Q. Xu, X. Wang, M. Xiao, Z. Zou, Hexahedron prism-anchored octahedronal CeO_2: crystal facet-based homojunction promoting efficient solar fuel synthesis, J. Am. Chem. Soc. 137 (2015) 9547–9550.
[78] W. Zou, Y. Shao, Y. Pu, Y. Luo, J. Sun, K. Ma, C. Tang, F. Gao, L. Dong, Enhanced visible light photocatalytic hydrogen evolution via cubic CeO_2 hybridized g-C_3N_4 composite, Appl. Catal. B Environ. 218 (2017) 51–59.